Targeting TACE-dependent EGFR ligand shedding in breast cancer

Paraic A. Kenny and Mina J. Bissell

Life Sciences Division, Lawrence Berkeley National Laboratory, University of California, Berkeley, California, USA.

The ability to proliferate independently of signals from other cell types is a fundamental characteristic of tumor cells. Using a 3D culture model of human breast cancer progression, we have delineated a protease-dependent autocrine loop that provides an oncogenic stimulus in the absence of proto-oncogene mutation. Targeting this protease, TNF-α–converting enzyme (TACE; also referred to as a disintegrin and metalloproteinase 17 [ADAM17]), with small molecular inhibitors or siRNAs reverted the malignant phenotype in a breast cancer cell line by preventing mobilization of 2 crucial growth factors, TGF-α and amphiregulin. We show that TACE-dependent ligand shedding was prevalent in a series of additional breast cancer cell lines and, in all cases examined, was amenable to inhibition. Using existing patient outcome data, we demonstrated a strong correlation between *TACE* and *TGFA* expression in human breast cancers that was predictive of poor prognosis. Tumors resulting from inappropriate activation of the EGFR were common in multiple tissues and were, for the most part, refractory to current targeted therapies. The data presented here delineate the molecular mechanism by which constitutive EGFR activity may be achieved in tumor progression without mutation of the EGFR itself or downstream pathway components and suggest that this important oncogenic pathway might usefully be targeted upstream of the receptor.

Introduction

Whether achieved by gene overexpression, mutation, or amplification, the ability to grow independently of signals from other cell types is a central feature of tumorigenesis, and the acquisition of self-sufficiency for growth signals is a critical rate-limiting transition in the evolution of a tumor cell (1, 2). Pathways downstream of EGFR play essential roles in cell proliferation and tissue homeostasis. Genetic ablation of this receptor or some of its ligands impairs mammary gland development (3, 4), and deregulated ErbB pathway signaling contributes to a significant proportion of human cancer cases, both in the breast and in other tissues (5). Thus, appropriate spatial and temporal regulation of EGFR signaling is crucial for correct mammary gland development and for the maintenance of mammary epithelial organization.

Here we used 3D culture models of breast epithelial cells to investigate the molecular determinants of constitutive growth factor receptor signaling and to evaluate the phenotypic consequences of targeting these processes. The HMT3522 breast cancer progression series originated from purified human breast epithelial cells derived from reduction mammoplasty (6). Early passages (S1 cells) became spontaneously immortalized, and continue to be nonmalignant but require exogenous EGF for proliferation (6); these cells retain the capacity to differentiate into growth-arrested, polarized acinar structures when cultured in 3D gels of laminin-rich extracellular matrix (lrECM) (7). When EGF was removed and cells were continuously passaged, an EGF-independent population emerged (S2 cells, premalignant) that, when repeatedly injected into mice, gave rise to a line (T4-2 cells) that is consistently tumorigenic in vivo (8, 9). These cells fail to arrest growth in the 3D assay and form large, continuously proliferating, apolar colonies. Compared with S1 cells, T4-2 cells express high levels of phosphorylated EGFR, and treatment of these cells in 3D cultures with inhibitors of components of this pathway elicits a striking morphological reversion leading to organized, growth-arrested, polarized structures resembling primary or S1 acini (7, 10).

We used this model to investigate the mechanisms by which nonmalignant breast epithelial cells escape dependence on exogenous EGF and eventually become malignant. Using DNA sequencing, we determined that T4-2 cells had not acquired mutations in common proto-oncogenes (*EGFR*, *H-Ras*, *K-Ras*, *N-Ras*, and *B-Raf*) but expressed 2 EGFR ligands, amphiregulin (AREG) and TGF-α, not present in S1 cells. A metalloproteinase, TNF-α–converting enzyme (TACE; also referred to as a disintegrin and metalloproteinase 17 [ADAM17]), implicated by others in processing of these ligands (11–14), was expressed in T4-2 cells and was necessary for AREG and TGF-α function. We found that inhibition of TACE using small molecules or siRNAs was sufficient to block EGFR signaling and to revert the malignant phenotype in T4-2 cells and that this was a direct consequence of attenuation of growth factor ectodomain shedding. We extended this analysis to several additional breast cancer cell lines and in all cases examined, TACE inhibition blocked the shedding of these EGFR ligands. Analysis of a published gene expression data set of 295 primary breast tumors and associated clinical data (15) revealed that TACE and TGF-α expression were highly correlated and predictive of a poor prognosis.

Our data provide additional insight into the mechanisms by which growth factor self-sufficiency can be achieved, a fundamental feature of tumorigenesis in the breast and other epithelial tissues, and suggest that targeting this ADAM-dependent autocrine loop may prove a useful therapeutic strategy for EGFR-dependent tumors of the breast and other tissues.

Results

AREG and TGFA are upregulated in T4-2 cells. The nonmalignant human breast epithelial cells in this model required exogenous

Nonstandard abbreviations used: ADAM, a disintegrin and metalloproteinase; AREG, amphiregulin; ERα, estrogen receptor α; lrECM, laminin-rich extracellular matrix; TACE, TNF-α–converting enzyme; TAPI-2, TNF protease inhibitor–2.

Conflict of interest: The authors have declared that no conflict of interest exists.

Citation for this article: *J. Clin. Invest.* **117**:337–345 (2007). doi:10.1172/JCI29518.

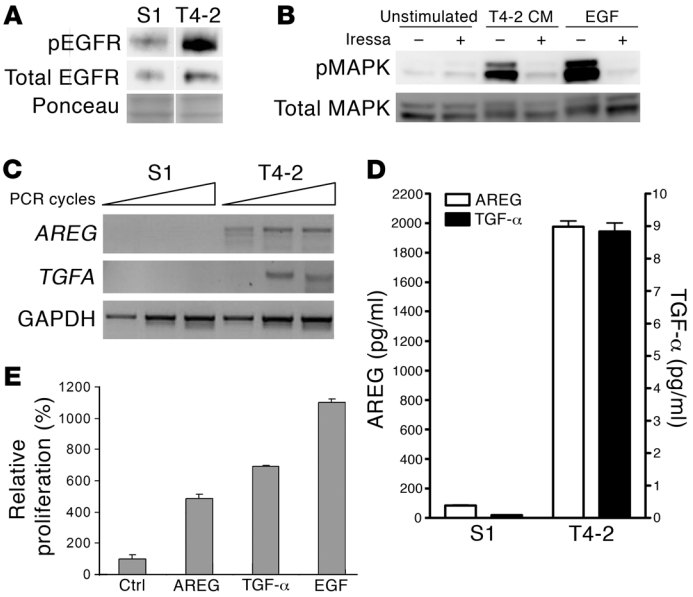

Figure 1
Upregulation of an autocrine growth factor loop during a model of breast cancer progression. (**A**) T4-2 (malignant) cells, which grow independently of exogenous EGF, had significantly higher activity of EGFR than their phenotypically normal counterpart, S1 (nonmalignant) cells. The level of EGFR phosphorylation is consistent with activation by a soluble factor produced in these cells. Ponceau S staining was used as a loading control. (**B**) S1 cells were starved of EGF for 12 hours and then stimulated for 10 minutes with either T4-2 conditioned medium (CM) or 5 ng/ml EGF. A 5 minute pretreatment with Iressa (0.3 nM) abolished MAPK activation induced by the conditioned medium and by EGF. (**C**) RT-PCR analysis shows that *AREG* and *TGFA* were transcriptionally upregulated in T4-2 relative to S1 cells. GAPDH was used as a loading control. (**D**) ELISA of conditioned medium shows that T4-2 cells secreted significantly more AREG and TGF-α than did S1 cells. (**E**) S1 cell proliferation in the presence of all EGFR ligands (860 pM) was significantly different from control (Ctrl).

EGF for proliferation (Figure 1E), while their malignant derivative, T4-2, acquired self-sufficiency for this signal. The sensitivity of T4-2 cells to inhibition of EGFR (10) implies that EGFR and the downstream components of the pathway are not constitutively activated. Using direct sequencing, we showed that these cells had not sustained activating mutations in *EGFR*, *H-Ras*, *K-Ras*, *N-Ras*, or *B-Raf* (data not shown). As previously described (10), T4-2 cells had significantly higher levels of active EGFR than did their S1 precursors (Figure 1A). Thus, we hypothesized that T4-2 cells have escaped dependence on exogenous EGF by transcriptionally upregulating one or more ErbB ligands. Conditioned medium from T4-2 cells elicited rapid activation of MAPK in S1 cells, which was comparable to that induced by exogenously added EGF (Figure 1B). While ligands of a number of receptor tyrosine kinases activate MAPK, the observed activation was suppressed by preincubation of S1 cells with the EGFR inhibitor gefitinib (Iressa, ZD1839; AstraZeneca). Thus we suspected that T4-2 cells produce one or more soluble EGFR ligands. We tested expression of the genes encoding AREG, Betacellulin, Cripto, EGF, Epiregulin, HB-EGF, NRG1, NRG2, and TGF-α by RT-PCR. *AREG* and *TGFA* were expressed at high levels in T4-2 cells (Figure 1C). Using ELISA, we confirmed the presence of AREG and TGF-α in the conditioned medium of T4-2 cells (Figure 1D). Adding concentrations of recombinant AREG or TGF-α equimolar to that of EGF to the medium of S1 cells (860 pM) showed that these ligands can substitute for EGF to promote proliferation of the nonmalignant cells (Figure 1E).

A metalloproteinase activity is critically required for mobilization of growth factors. Several growth factors, including AREG and TGF-α, are synthesized as transmembrane precursors and are processed by the members of the ADAM family of transmembrane proteases (11–13). Culture of T4-2 cells in 3D laminin-rich gels resulted in the formation of disorganized, apolar, continuously proliferating colonies (Figure 2A), a phenotype we have previously shown to be highly correlated with, and reflective of, the ability of cancer cells to form tumors in vivo (7, 16). Incubation with TNF protease inhibitor–2 (TAPI-2), a broad-spectrum inhibitor of MMPs and ADAMs, resulted in a reversion of the malignant phenotype (Figure 2C) similar to that elicited using the EGFR inhibitor AG1478 (Figure 2B), suggesting that a metalloproteinase activity is required for the proliferative phenotype of T4-2 cells. This treatment also resulted in the restoration of epithelial polarity. Vehicle-treated cells remained disorganized (Figure 2D), whereas TAPI-2–treated cells assumed a polar organization reminiscent of breast acini, here indicated by basal localization of α_6 integrin (Figure 2E). The colonies formed by AG1478- or TAPI-2–treated T4-2 cells were similar in size to nonmalignant mammary acini and were significantly smaller than those formed by cells treated with vehicle alone (Figure 2F).

T4-2 cells exhibited a basal level of signaling kinase activity downstream of the EGFR (Figure 2G), consistent with a response to the ongoing production of an EGFR ligand by these cells. The basal activities were significantly suppressed by addition of TAPI-2, but the cells remained competent to respond to addition of exogenous EGF (Figure 2G). Furthermore, TAPI-2 caused a dose-dependent decrease in proliferation of T4-2 cells in 2D cultures, which was also overcome by addition of exogenous EGF (Figure 2H). This compound was not cytotoxic at the concentration used, nor did it interfere with the ability of S1 cells to execute normal acinar morphogenesis in the presence of soluble EGF (data not shown). Thus, the proliferative block and concomitant reversion resulting from metalloproteinase inhibition appeared to result from a defect in growth factor mobilization, which was confirmed by ELISA analysis (Figure 2I).

TACE cleaves both AREG and TGF-α in cultured mammary epithelial cells. Several lines of genetic and biochemical evidence suggest that TACE is a key regulator of cleavage of AREG as well as TGF-α (11–13, 17). TACE is expressed in both S1 and T4-2 cells (Figure 3A). To test whether TACE is the key sheddase for these endogenously produced growth factors in these cells, we used siRNA to knock down expression of TACE and measured growth factor shedding from the transfected cells (Figure 3B). The 3 siRNAs used against TACE suppressed its expression with varying degrees of efficacy. The most effective, siTACE-1, caused a dramatic decrease in the shedding of both ligands, whereas cells transfected with the less effective siRNAs retained the ability to shed ligands in proportion to the amount of TACE expressed. Introduction of the most effective siRNA against TACE (Figure 3C) had no apparent effect

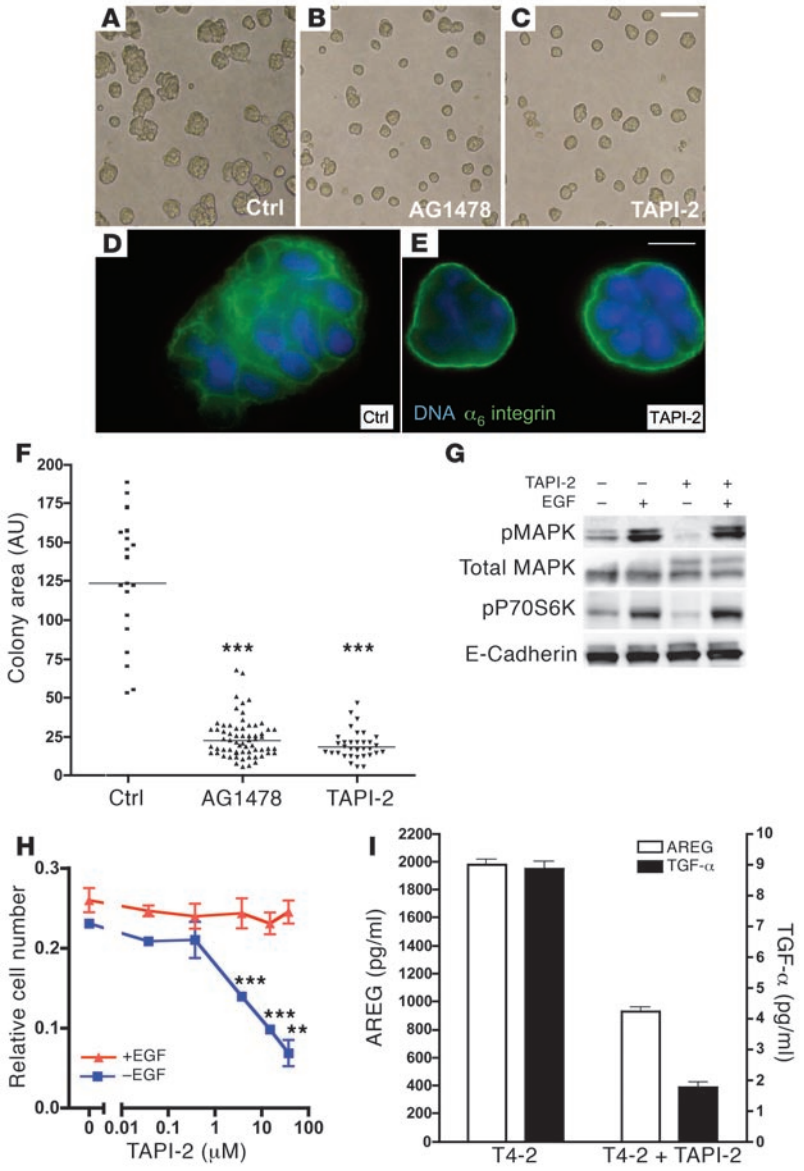

Figure 2
Inhibition of sheddase activity reverts the malignant phenotype of T4-2 cells by suppressing mobilization of growth factors and downregulating EGFR pathway activity. (**A**) T4-2 cells grown in 3D lrECM cultures formed continuously proliferating, disorganized, apolar colonies. (**B**) T4-2 cells treated with EGFR inhibitor (80 nM AG1478) underwent morphological reversion, forming small, smooth, spherical, growth-arrested colonies. (**C**) T4-2 cells treated with a broad-spectrum MMP/ADAM inhibitor (20 μM TAPI-2) underwent morphological reversion similar to that of EGFR inhibitor–treated cells. (**D**) Absence of tissue polarity as demonstrated by α_6 integrin staining of vehicle-treated T4-2 cells. (**E**) Restoration of tissue polarity as demonstrated by α_6 integrin staining of TAPI-2–treated T4-2 cells. Scale bars: 100 μm (**A**–**C**); 10 μm (**D** and **E**). (**F**) Analysis of cross-sectional area of T4-2 cells treated with either vehicle, AG1478, or TAPI-2 for 4 days. ***P < 0.001 versus control. (**G**) TAPI-2 treatment (24 hours) reduced the basal activity of kinases downstream of EGFR, but cells remained competent to respond to exogenous EGF (860 pM, 5-minute stimulation). (**H**) TAPI-2 treatment resulted in a dose-dependent reduction in T4-2 cell proliferation that was completely overcome by addition of soluble EGF. **P < 0.01; ***P < 0.001 compared with 0 μM TAPI-2. (**I**) ELISA of conditioned medium from TAPI-2–treated T4-2 cells, indicating that it suppressed the shedding of both AREG and TGF-α.

on the morphology of cells cultured on plastic, but resulted in a dramatic reversion of the malignant phenotype of T4-2 cells in 3D lrECM culture compared with the random siRNA–transfected control. The shedding of both EGFR ligands was significantly reduced in these cultures (Figure 3D). Thus it appears that TACE, and not another TAPI-2–sensitive protease, is the primary growth factor sheddase in the T4-2 breast cancer cell line.

AREG and TGF-α are the key substrates of TACE in T4-2 cells. In addition to shedding growth factors, TACE has been implicated in the shedding of several other cell surface molecules, the inhibition of which might also contribute to the observed reversion of the T4-2 cell phenotype. Characterized substrates of TACE include TNF-α (18, 19), L selectin and TNFRII (20), β-APP (21), collagen XVII (22), growth hormone receptor (23), TrkA (24), ErbB4 (25), and GPIbα (26). To test whether modulation of growth factor cleavage is the key role of TACE and whether overexpression of these substrates leads to a genetic rescue of the TAPI-2–imposed reversion, we generated soluble secreted mutants of AREG and TGF-α lacking both the transmembrane and the cytosolic domains (AREGΔTM and TGF-αΔTM, respectively; Figure 4A). Whereas each stably infected T4-2 cell line was susceptible to reversion by EGFR inhibition (Figure 4B), those cells that produced soluble growth factors were completely resistant to TAPI-2 by criteria of colony size and morphology (Figure 4, B and C). Much like the parental cells, they continued to proliferate and formed disorganized, nonpolarized colonies (Figure 4D). Thus, despite the number of TACE substrates expressed by these cells, it is the suppression of growth factor mobilization that results in the reversion of the malignant phenotype.

TACE inhibition reduces EGFR ligand shedding in several breast cancer cell lines. To test whether our observations were generalizable, we screened several additional breast cancer cell lines to identify those that secrete either AREG or TGF-α. AREG was secreted by MCF-7, HCC1500, and ZR75B cells, while TGF-α was secreted by HCC1500 and MDA-MB-468 cells. In each case, 20 μM TAPI-2 significantly reduced ligand shedding from these cells (Figure 5, A and B). Transfection of MCF-7 cells with the siRNA against TACE led to a reduction in AREG shedding by 90%, indicating that, as with T4-2 cells, TACE is the key sheddase in this cell line (data not shown). We examined the activity of the EGFR pathway in these cell lines treated with TAPI-2 for 1 or 5 hours and found significant downregulation of MAPK activity in those cells expressing high levels of EGFR (Figure 5C). These data indicate that TACE-dependent growth factor shedding is common, at least in established breast cancer cell lines, and that it is amenable to therapeutic intervention.

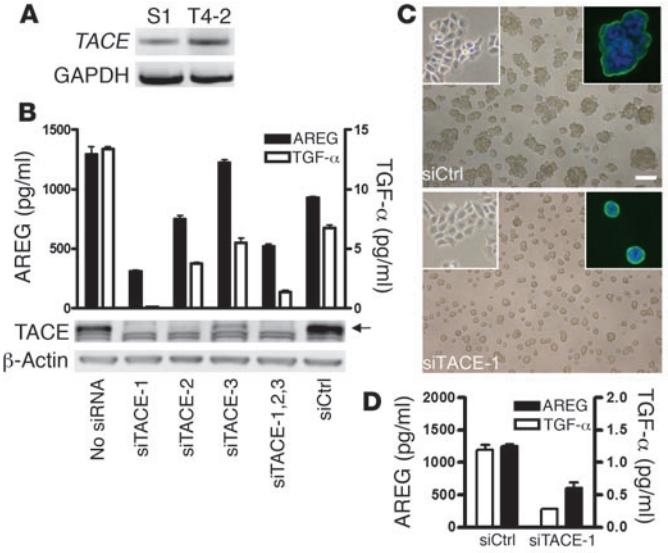

Figure 3
TACE cleaves AREG and TGF-α and is necessary for T4-2 cell proliferation. (**A**) RT-PCR analysis showing *TACE* expression in S1 and T4-2 cells. GAPDH was used as a loading control. (**B**) ELISA analysis of EGFR ligand shedding in T4-2 cells transfected with 3 siRNA oligos, either individually or as a pool. Ligand shedding was proportional to the level of TACE expression. (**C**) Reversion of the malignant phenotype of T4-2 cells in 3D lrECM culture following transfection of siRNA against TACE. Left insets: Phase-contrast micrographs of transfected cells grown on plastic. Right insets: α_6 integrin immunostaining of representative colonies. Original magnification, ×100; ×600 (right insets). (**D**) ELISA analysis of the conditioned medium from the experiment shown in **C**.

TACE and TGFA predict poor prognosis in human breast cancer patients. Having thus established that TACE-dependent growth factor shedding plays a role that is both critically important and therapeutically tractable in the HMT3522 model of breast cancer progression and demonstrated its prevalence in other breast cancer models, we sought to determine the extent to which these factors play a role in human breast cancer. We interrogated a comprehensive gene expression microarray data set of 295 primary human breast tumors prepared by van de Vijver and colleagues, who used it to identify gene expression signatures predictive of outcome (15). The detailed clinical characteristics of these tumors have been reported but briefly: all were either stage I or II, less than 5 cm in diameter at excision, and derived from 295 consecutively treated patients less than 53 years old. Approximately three-quarters of the tumors were estrogen receptor α (ERα) positive, and half were associated with positive lymph nodes. The median time for which follow-up information is available is 10.2 years (range, 0.05–21.6 years).

Our analysis of this data set revealed a statistically significant positive correlation between expression levels of *TGFA* and *TACE* ($P < 0.001$; Table 1). *EGFR* expression also correlated with both *TGFA* and *TACE*, although not at the level of statistical significance ($P = 0.053$ and $P = 0.061$, respectively). Unexpectedly, AREG expression in this patient population was inversely correlated with expression of *EGFR* and *TGFA* ($P < 0.05$ and $P < 0.001$, respectively). *AREG* and *TACE* levels tended to be inversely correlated as well, although not reaching statistical significance ($P = 0.053$). The explanation appears to involve the subtype of breast cancers examined. Tumors positive for *TGFA*, *TACE*, and *EGFR* were essentially *ERα* negative ($P < 0.0001$, $P < 0.005$, and $P < 0.0001$, respectively). Conversely, *ERα*-positive tumors had higher levels of *AREG* ($P < 0.0001$). We stratified the tumors into the standard subtypes (Basal, ErbB2, Luminal A, Luminal B, and Normal breast–like; ref. 27) to determine whether tumors expressing high levels of either growth factor were overrepresented in a particular subtype (Supplemental Table 1; supplemental material available online with this article; doi:10.1172/JCI29518DS1). These data indicate that the tumors with the highest levels of *TGFA* and *TACE* were overrepresented in the basal subtype, while tumors expressing high levels of AREG were predominantly found in the normal breast–like subgroup. The data also suggest that TACE and TGF-α may be the more important protease/growth factor pair for EGFR activation in human breast tumors (see Discussion).

To analyze the contribution of *AREG*, *TGFA*, and *TACE* expression to survival of human breast cancer patients, tumors were divided in quartiles by expression level of each marker, and survival curves were computed for the upper and lower quartiles (74 samples each) and the interquartile range (147 samples). Survival was evaluated at 5 and 10 years after surgery. High levels of *TACE* expression were associated with poor survival (Figure 6A), as were high levels of *TGFA* (Figure 6B). Tumors that expressed high levels of *AREG*, however, had a better outcome than those with lower *AREG* expression ($P < 0.005$, Figure 6C), as expected based on the high correlation between *AREG* and *ERα* expression levels. Of the 74 tumors with the highest levels of *AREG* expression, 73 were *ERα*-positive, i.e., only 1 *AREG*-high tumor was ERα negative. While a positive association between an EGFR ligand and good outcome may at first appear counterintuitive, it is important to note that these survival figures do not represent the natural course of the disease: they represent the course of the disease following treatment. Because of the success of tamoxifen in patients with ERα-positive tumors, it is unsurprising that *AREG* correlates with survival — it appears to be a marker for ERα-positive breast tumors, which have a relatively good prognosis because of the use of this drug (Figure 6D).

These data shed light at a molecular level on the steps by which tumor cells may become independent of extrinsic proliferative signals and suggest that targeting ADAM family members may be a useful strategy for treating EGFR-dependent tumors of the breast and other tissues.

Discussion

In this study, we used 3D ECM-based assays to delineate the mechanisms driving the activation of the EGFR in a progression model of human breast cancer and to demonstrate that these factors are amenable to therapeutic targeting. We showed that activation of EGFR signaling in the malignant T4-2 cells of the HMT3522 breast cancer progression series was driven by a TACE-dependent growth factor autocrine loop not present in the non-

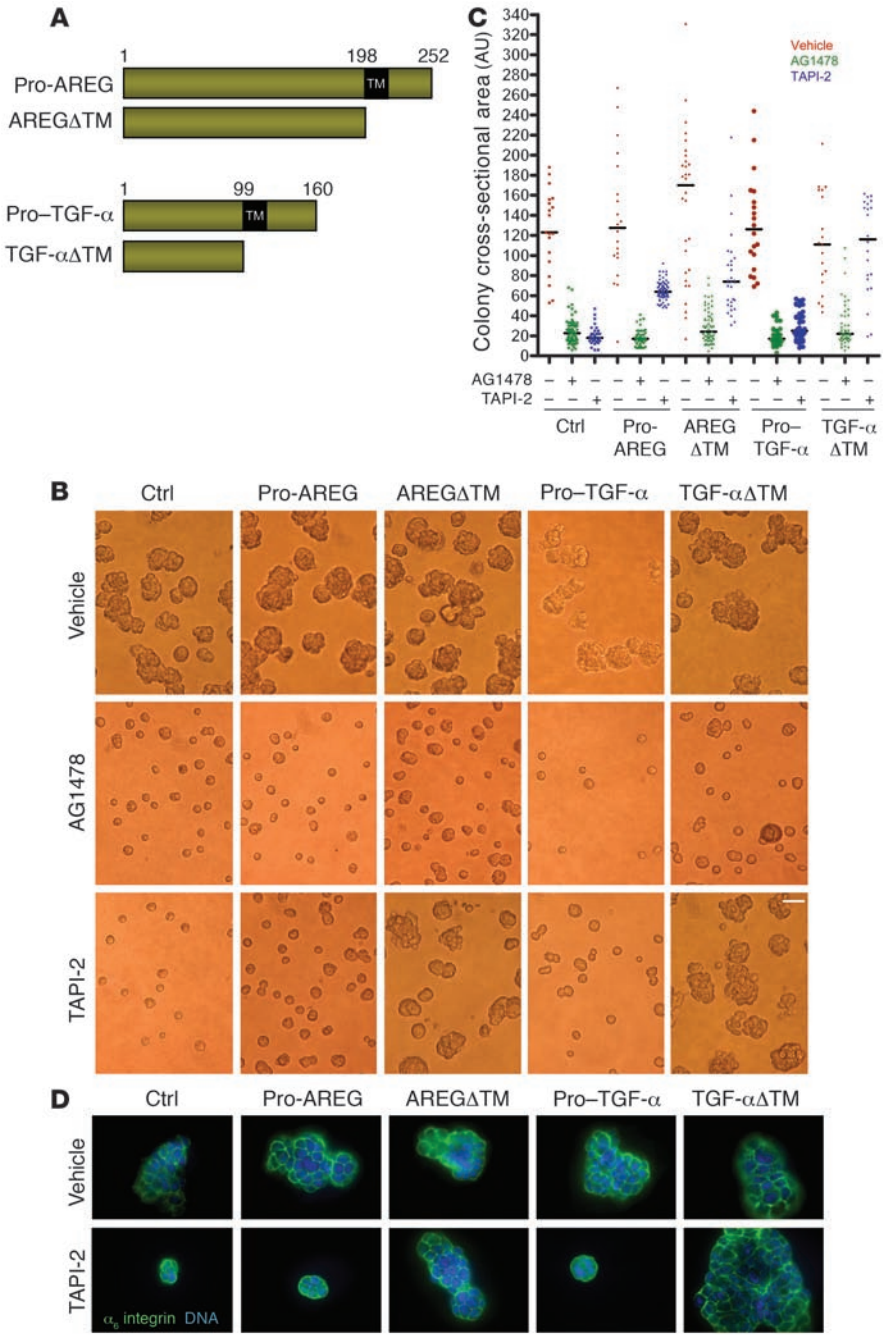

Figure 4
TAPI-2–induced reversion of T4-2 cells is a direct result of inhibition of growth factor ectodomain shedding. (**A**) Schematic representation of full-length (pro-) and deletion mutants (ΔTM) of AREG and TGF-α. Deletion mutants lack both the transmembrane and the cytoplasmic domains and can thus be secreted without requiring TACE activity. (**B**) T4-2 cells overexpressing full-length or deletion growth factor constructs were susceptible to reversion by the EGFR inhibitors, but cells expressing either soluble AREG or soluble TGF-α escaped the TAPI-2–induced reversion. Scale bar: 100 μm. (**C**) Analysis of cross-sectional area of T4-2 cells and derivatives in response to pharmacological inhibition of EGFR and TACE. Horizontal bars represent median values. (**D**) Higher-magnification (×600) analysis of representative colonies from **B**. Colonies expressing the soluble mutants of AREG and TGF-α remain disorganized and apolar in the presence of TAPI-2.

malignant S1 cells. Inhibition of TACE attenuated the growth of T4-2 cells in 3D ECM culture and reverted their morphology to approximate that of nonmalignant cells. This reversion was overcome by overexpression of soluble precleaved mutants of either AREG or TGF-α but not by full-length AREG or TGF-α, demonstrating definitively the importance of growth factor precursor cleavage for ErbB function. In all of the breast cancer cell lines in which we detected shedding of these EGFR ligands, we succeeded in reducing their production by TACE inhibition.

In human breast cancer patients, we further showed that expression of TACE and TGF-α was highly correlated and predictive of poor prognosis, suggesting that TACE inhibition might provide a clinical benefit in this population. Conversely, expression of AREG in this patient population was associated with good outcome. While the latter finding may appear counterintuitive in light of our results in culture, it is consistent with our current understanding of the mechanisms by which AREG expression is regulated. AREG was first identified in an ERα-positive breast cancer cell line (28). Its expression is known to be both estrogen responsive and repressible by antiestrogens (29). The gene expression profiles in our study represent a snapshot of these tumors at the time of surgical excision (and, of course, before adjuvant tamoxifen was given). The exquisite dependence of ERα-positive breast cancers on hormonal stimulation for their induction,

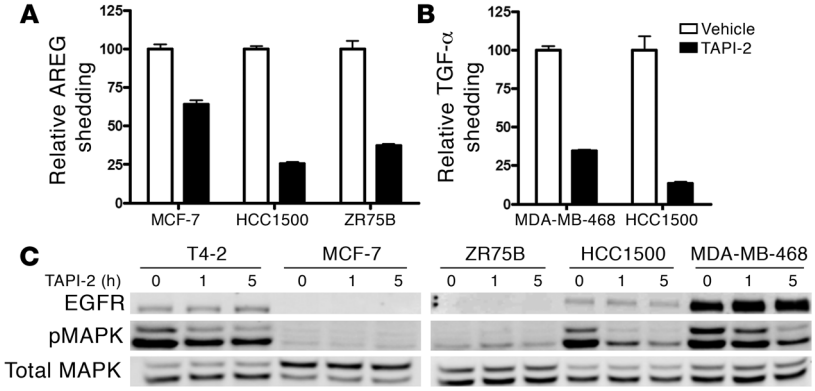

Figure 5
Suppression of growth factor shedding by TAPI-2 in a panel of breast cancer cell lines. (**A**) Three AREG-expressing breast cancer lines were treated with 20 μM TAPI-2 or vehicle for 90 minutes, and AREG shedding was quantified by ELISA. (**B**) Two breast cancer cell lines expressing TGF-α were identified and treated as in **A**, and TGF-α shedding was quantified by ELISA. TAPI-2 suppressed TGF-α shedding. (**C**) Each cell line was treated with TAPI-2 for either 1 or 5 hours. Downregulation of MAPK activity was detected in those cell lines expressing EGFR.

maintenance, and progression has been very well established for many decades and forms the basis of several successful breast cancer therapies: first surgical oophorectomy, then tamoxifen, and more recently the aromatase inhibitors anastrazole, exemesthane, and letrozole. It is thus unsurprising that Cox proportional hazard regression modeling in this population indicates that *AREG* does not predict survival *independently* of hormone receptor status, as ERα positivity conferred a survival benefit (relative risk [RR] of death, 0.46; 95% confidence interval [CI], 0.27–0.71) and *AREG* was not an independent prognostic indicator as its 95% CI included 1 (RR, 0.60; 95% CI, 0.34–1.05).

The mechanism by which TACE is regulated in the HMT3522 model remains unclear. While it is expressed at broadly similar levels in these cell lines, it appears to be more active in T4-2 cells. Preliminary experiments to measure potential negative regulators of TACE activity suggested that at least one inhibitor, tissue inhibitor of metalloproteinase 3 (TIMP3), is expressed at similar levels in each line (data not shown). TACE can also be positively regulated by G protein–coupled receptors (12, 30), one or more of which may have been induced during the transition to EGFR signaling self-sufficiency in this model. Although G protein–coupled receptors have been implicated pharmacologically in the stimulation of TACE-dependent ectodomain shedding (12, 30), the identities of the individual receptors involved remain largely unknown.

Despite the development of potent, specific EGFR inhibitors, EGFR-dependent tumors of several tissues remain a substantial clinical problem. Small-molecule inhibitors of the EGFR have thus far proven disappointing in phase III clinical trials. Like AG1478, Iressa and erlotinib (Tarceva, OSI-774; Genetech Inc.) are reversible anilinoquinazoline derivatives. In 2 large trials of non–small cell lung cancer (NSCLC) patients, chemotherapy with Iressa performed no better than chemotherapy alone in terms of survival (31, 32). Although Tarceva did provide a statistically significant survival benefit in patients with advanced pancreatic adenocarcinoma, it is important to note that the median extension in progression-free survival was a mere 6 days, while the median increase in overall survival was 14 days (33). In a recent trial using Tarceva as a single agent in NSCLC, median progression-free survival time was increased by less than 2 weeks in the treated population, while median overall survival was increased by 2 months (34). Some patients who have responded to therapy have had tumors bearing EGFR mutations (35, 36), but this explains only a proportion of responses in these studies, and the association has not been reproduced in another large study (37).

The demonstration of an absolute requirement for the proteolytic activity of TACE for growth factor shedding and proliferation in a physiologically relevant model of human breast cancer progression suggests another possible avenue to be explored therapeutically. MMPs and ADAMs have been studied intensively and many small-molecule inhibitors have been characterized in both cell culture and animal models, primarily to inhibit MMP-dependent tumor cell invasion. Despite the relative success of preclinical studies, the results of many clinical trials of MMP inhibitors in cancer have been disappointing, perhaps due to what retrospectively appears to be flawed design of the phase III studies (38). It has become clear that metalloproteinases play more complex and diverse roles in tumor progression (39) than was appreciated during the design of these earlier clinical studies. It remains possible that these compounds may prove efficacious in selected subsets of patients, one such cohort being those who depend on TACE-dependent autocrine stimulation of EGFR/ErbB2. Specific and orally active TACE inhibitors have been developed by Roche Diagnostics (40) and Wyeth (41) for treatment of arthritis (TACE also cleaves TNF-α, an important proinflammatory cytokine in this disease). Our data suggest that their efficacy should be evaluated in a preclinical model of EGFR ligand–dependent tumorigenesis.

Table 1
Pearson's correlation analysis of markers in 295 primary human breast tumors

	AREG	*ERα*	*TGFA*	*TACE*	*EGFR*
ERα	0.4177 ($P < 0.0001$)				
TGFA	–0.2155 ($P = 0.0002$)	–0.3851 ($P < 0.0001$)			
TACE	–0.1126 ($P = 0.0534$)	–0.1774 ($P = 0.0022$)	0.1917 ($P = 0.0009$)		
EGFR	–0.1416 ($P = 0.0150$)	–0.2755 ($P < 0.0001$)	0.1127 ($P = 0.0532$)	0.1093 ($P = 0.0609$)	
ErbB2	0.1897 ($P = 0.0011$)	–0.0943 ($P = 0.1062$)	–0.1027 ($P = 0.0783$)	–0.0340 ($P = 0.5609$)	–0.0557 ($P = 0.3407$)

Values represent Pearson's *r*.

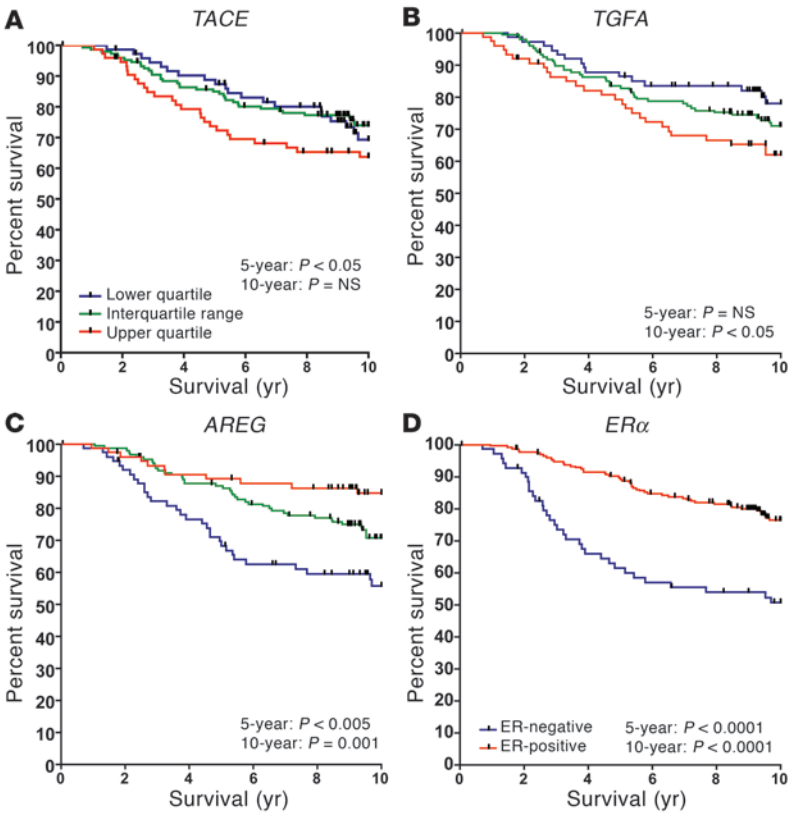

Figure 6
Kaplan-Meier survival analysis of 295 human breast tumors stratified by marker expression level. High levels of (**A**) *TACE* and (**B**) *TGFA* predict poor survival. High levels of (**C**) *AREG* or (**D**) *ERα* are correlated with good outcome (*AREG* and *ERα* are related; see Discussion). *P* values represent the log-rank comparison between the upper and lower quartiles of marker expression evaluated at 5 and 10 years after surgery.

Data from the phase I studies indicate that these selective drugs produce relatively few side effects compared with the first-generation MMP inhibitors, for which dose-limiting toxicity proved to be a major clinical problem.

The data delineate further a mechanism by which breast epithelial cells may escape dependence on extrinsic proliferative signals, a transition necessary in the evolution of all cancers. TACE appears to play an essential role in this escape. Inhibition of this protease blocked EGFR signaling and reverted the malignant phenotype, suggesting that interruption of such an autocrine loop, either with a single agent or in combination with existing EGFR inhibitors, might prove an effective therapy for tumors dependent on EGFR ligand expression.

Methods

Cell culture. All reagents were purchased from Sigma-Aldrich except where otherwise noted. HMT3522 cells were cultivated on 2D and 3D substrata in H14 medium, a 50:50 mix of DMEM/F12 (UCSF Cell Culture Facility) supplemented with 5 μg/ml prolactin, 250 ng/ml insulin, 1.4×10^{-6} M hydrocortisone, 10^{-10} M β-estradiol, 2.6 ng/ml sodium selenite, and 10 μg/ml transferrin. S1 cells were additionally supplemented with 10 ng/ml EGF. In various experiments, cells were supplemented with AREG, TACE, and TGF-α. In all cases, AREG and TGF-α were used at the same molar concentration as EGF (860 pM).

For 3D lrECM culture, T4-2 cells were seeded at 21,000 cells per cm^2 on top of Matrigel, overlaid with H14 medium containing 5% Matrigel (BD Biosciences), and treated with 80 nM AG1478, 20 μM TAPI-2, 0.3 nM Iressa, or the relevant vehicle controls.

Amphotropic retroviruses were generated by transfection (Lipofectamine; Invitrogen) of the Phoenix packaging cell line (a gift of G. Nolan, Stanford University, Stanford, California, USA) with pBM-IRES-puro or derivatives containing the AREG or TGF-α open reading frames. We plated 2×10^6 phoenix cells per 6-cm dish and on the following day transfected them with 2 μg of the appropriate retroviral construct. Retrovirus-containing culture medium was harvested after 48 hours, supplemented with polybrene to 5 μg/ml, and added to HMT3522 cells at 30%–50% confluence. Pools of stable infectants were selected in 1 μg/ml puromycin.

Silencer siRNAs against TACE (Ambion) were transfected in according to the reverse transfection protocol of Invitrogen. siRNAs against the following TACE sense strand sequences were transfected either individually (100 nM) or as a pool (33.3 nM each): CCAGAGACUCGAGAAGCUUTT, GCAGCAUUCGGUAAGAAAATT, and CGAGAACAAUAAGAUGUUUTT. For 3D culture assays, T4-2 cells were trypsinized after transfection and plated as single cells in Matrigel. Knockdown was assessed by Western blot from a parallel transfection 48 hours after transfection. Random siRNA sequence was used as a negative control.

Indirect immunofluorescence. Colonies were solubilized from Matrigel culture by shaking in PBS with 0.05 M EDTA on ice for 30 minutes, fixed in 1:1 methanol/acetone at –20°C, stained with anti–α_6 integrin (Chemicon International), and counterstained with DAPI.

Western blotting. Cells were lysed in 50 mM Tris-HCl (pH 7.5), 150 mM NaCl, 0.5% NP-40 supplemented with protease and phosphatase inhibitors (Calbiochem) and clarified by centrifugation. We fractionated 50 μg of each sample by SDS-PAGE, transferred them to nitrocellulose membranes, and probed them with antibodies against the following proteins: phosphorylated MAPK, total MAPK, phosphorylated p70S6 kinase (Cell Signaling Technology), and TACE (Chemicon International). E-cadherin (BD Biosciences) was used as a loading control. Blots were developed using SuperSignal West Femto chemiluminescence reagent (Pierce Biotechnology). Images were captured using a FluorChem 8900 imager (Alpha Innotech).

ELISA. Equal numbers of cells were washed 3 times and allowed to condition medium for 90 minutes. The amount of AREG and TGF-α accumulating in the medium was determined by using specific ELISA assays (R&D Systems) according to the manufacturer's instructions.

Cloning of full-length AREG and TGF-α. The open reading frames of these genes were amplified by PCR from T4-2 cDNA. Amplification products were cloned, sequence verified, and subcloned into the retroviral expression vector pBM-IRES-puro (42). The primers used were as follows: AREG, 5′-GACCTCAATGACACCTACTCTGG-3′ and 5′-GAAATATTCTTGCTGACATTTGC-3′; TGF-α, 5′-ATGGTCCCCTCGGCTGGACAGCTC-3′ and 5′-TCATAGATCTTCTTCTGATATAAGCTTTTGTTCGACCACTGTTTCTGAGTGGC-3′. The mutants of AREG and TGF-α were generated using the pBM-IRES-puro–specific primer 5′-TGGAAAGGACCTTACACAGTCC-3′ and either 5′-AAAAGGATCCTCATTTTGATAAACTACTGTCAATC-3′ (AREGΔTM) or 5′-AAAAGGATCCTCAGGCCTGCTTCTTCTGGCTGGC-3′ (TGF-αΔTM) and cloned into pBM-IRES-puro.

Proliferation assays. HMT3522 cells were seeded in 48-well plates and treated (in triplicate) as described in the figure legends. To determine relative growth, 0.1 volumes of WST cell proliferation analysis reagent (Roche Diagnostics) was added to the medium, and its formazan metabolite was measured by absorbance at 460 nm.

Quantitation of colony size in the 3D lrECM culture was performed by image analysis. Representative images were captured using a digital camera (Nikon Coolpix 4500) attached to a phase-contrast microscope (Nikon Eclipse TS100). The high-resolution digital images were then analyzed using NIH ImageJ software (version 1.36b; http://rsb.info.nih.gov/nih-image/), and the cross-sectional area of each colony was determined for many colonies. This process was hand-curated to ensure that aggregates of colonies were not measured as a single colony.

RT-PCR. DNase-treated total RNA was isolated using the RNeasy Mini kit (QIAGEN). We used 5 μg of total RNA in a final volume of 40 μl for oligo dT–primed cDNA synthesis (First Strand cDNA Synthesis Kit; Invitrogen). Primers used were as follows: AREG, 5′-GACCTCAATGACACCTACTCTGG-3′ and 5′-GAAATATTCTTGCTGACATTTGC-3′; GAPDH, 5′-CCCCTGGCCAAGGTCATCCATGAC-3′ and 5′-CATACCAGGAAATGAGCTTGACAAAG-3′; TACE, 5′-CAGCACAGCTGCCAAGTCATT-3′ and 5′-CCAGCATCTGCTAAGTCACTTCC-3′; TGF-α, 5′-CACACTCAGTTCTGCTTCCA-3′ and 5′-TCAGACCACTGTTTCTGAGTGGC-3′.

Statistics. All data analysis was performed using GraphPad Prism version 4.03. Bar graphs represent mean ± SEM. Significance was determined using ANOVA. In scatter plots, the horizontal bar represents the median of each data set. Significance was determined using the Kruskal-Wallis test (with Dunn's test to correct for multiple comparisons).

A gene expression database consisting of the microarray profiles of 295 human breast tumors with the associated clinical data (15) was obtained from Rosetta Inpharmatics. Pearson's correlation coefficient was used to determine whether statistically significant associations existed between the relative expression levels of each of the markers. For survival analysis, patients were stratified into quartiles for expression of each marker, and survival curves were computed using the method of Kaplan and Meier. Statistical significance was determined using the log-rank test. A P value of less than 0.05 was considered statistically significant.

Acknowledgments

We thank Derek Radisky for critical reading of the manuscript and helpful suggestions; Jimmie Fata, Mark Sternlicht, and Mathew Coleman for stimulating discussions; and Dinah Levy and Christiane Abouzeid for excellent technical assistance. We gratefully acknowledge Dimitry Nuyten of the Netherlands Cancer Institute for sharing the latest follow-up data on the 295-patient data set in advance of publication. These investigations were supported by grants and a Distinguished Fellowship Award from the US Department of Energy, Office of Biological and Environmental Research (DE-AC03 SF0098), by the National Cancer Institute (2 R01 CA064786-09), and by an Innovator Award from the Department of Defense Breast Cancer Research Program (BC012005) to M.J. Bissell. P.A. Kenny was supported by fellowships from the Susan G. Komen Breast Cancer Foundation (#2000-223) and the Department of Defense Breast Cancer Research Program (DAMD17-00-1-0224).

Received for publication June 26, 2006, and accepted in revised form November 21, 2006.

Address correspondence to: Paraic A. Kenny or Mina J. Bissell, Life Sciences Division, Lawrence Berkeley National Laboratory, 1 Cyclotron Road MS977-225A, University of California, Berkeley, California 94720, USA. Phone: (510) 486-4365; Fax: (510) 486-5586; E-mail: pakenny@lbl.gov (P.A. Kenny). E-mail: mjbissell@lbl.gov (M.J. Bissell).

1. Bissell, M.J., et al. 1999. Tissue structure, nuclear organization, and gene expression in normal and malignant breast. *Cancer Res.* **59**(7 Suppl.):1757s–1763s; discussion 1763s–1764s.
2. Hanahan, D., and Weinberg, R.A. 2000. The hallmarks of cancer. *Cell.* **100**:57–70.
3. Wiesen, J.F., Young, P., Werb, Z., and Cunha, G.R. 1999. Signaling through the stromal epidermal growth factor receptor is necessary for mammary ductal development. *Development.* **126**:335–344.
4. Luetteke, N.C., et al. 1999. Targeted inactivation of the EGF and amphiregulin genes reveals distinct roles for EGF receptor ligands in mouse mammary gland development. *Development.* **126**:2739–2750.
5. Downward, J. 2003. Targeting RAS signalling pathways in cancer therapy. *Nat. Rev. Cancer.* **3**:11–22.
6. Briand, P., Petersen, O.W., and Van Deurs, B. 1987. A new diploid nontumorigenic human breast epithelial cell line isolated and propagated in chemically defined medium. *In Vitro Cell. Dev. Biol.* **23**:181–188.
7. Petersen, O.W., Ronnov-Jessen, L., Howlett, A.R., and Bissell, M.J. 1992. Interaction with basement membrane serves to rapidly distinguish growth and differentiation pattern of normal and malignant human breast epithelial cells. *Proc. Natl. Acad. Sci. U. S. A.* **89**:9064–9068.
8. Briand, P., Nielsen, K.V., Madsen, M.W., and Petersen, O.W. 1996. Trisomy 7p and malignant transformation of human breast epithelial cells following epidermal growth factor withdrawal. *Cancer Res.* **56**:2039–2044.
9. Weaver, V.M., et al. 1997. Reversion of the malignant phenotype of human breast cells in three-dimensional culture and in vivo by integrin blocking antibodies. *J. Cell Biol.* **137**:231–245.
10. Wang, F., et al. 1998. Reciprocal interactions between beta1-integrin and epidermal growth factor receptor in three-dimensional basement membrane breast cultures: a different perspective in epithelial biology. *Proc. Natl. Acad. Sci. U. S. A.* **95**:14821–14826.
11. Borrell-Pages, M., Rojo, F., Albanell, J., Baselga, J., and Arribas, J. 2003. TACE is required for the activation of the EGFR by TGF-alpha in tumors. *EMBO J.* **22**:1114–1124.
12. Gschwind, A., Hart, S., Fischer, O.M., and Ullrich, A. 2003. TACE cleavage of proamphiregulin regulates GPCR-induced proliferation and motility of cancer cells. *EMBO J.* **22**:2411–2421.
13. Sahin, U., et al. 2004. Distinct roles for ADAM10 and ADAM17 in ectodomain shedding of six EGFR ligands. *J. Cell Biol.* **164**:769–779.
14. Zhou, B.B., et al. 2006. Targeting ADAM-mediated ligand cleavage to inhibit HER3 and EGFR pathways in non-small cell lung cancer. *Cancer Cell.* **10**:39–50.
15. van de Vijver, M.J., et al. 2002. A gene-expression signature as a predictor of survival in breast cancer. *N. Engl. J. Med.* **347**:1999–2009.
16. Wang, F., et al. 2002. Phenotypic reversion or death of cancer cells by altering signaling pathways in three-dimensional contexts. *J. Natl. Cancer Inst.* **94**:1494–1503.
17. Sternlicht, M.D., et al. 2005. Mammary ductal morphogenesis requires paracrine activation of stromal EGFR via ADAM17-dependent shedding of epithelial amphiregulin. *Development.* **132**:3923–3933.
18. Moss, M.L., et al. 1997. Cloning of a disintegrin metalloproteinase that processes precursor tumour-necrosis factor-alpha. *Nature.* **385**:733–736.
19. Black, R.A., et al. 1997. A metalloproteinase disintegrin that releases tumour-necrosis factor-alpha from cells. *Nature.* **385**:729–733.
20. Peschon, J.J., et al. 1998. An essential role for ect-

odomain shedding in mammalian development. *Science.* **282**:1281–1284.
21. Buxbaum, J.D., et al. 1998. Evidence that tumor necrosis factor alpha converting enzyme is involved in regulated alpha-secretase cleavage of the Alzheimer amyloid protein precursor. *J. Biol. Chem.* **273**:27765–27767.
22. Franzke, C.W., et al. 2002. Transmembrane collagen XVII, an epithelial adhesion protein, is shed from the cell surface by ADAMs. *EMBO J.* **21**:5026–5035.
23. Zhang, Y., Jiang, J., Black, R.A., Baumann, G., and Frank, S.J. 2000. Tumor necrosis factor-alpha converting enzyme (TACE) is a growth hormone binding protein (GHBP) sheddase: the metalloprotease TACE/ADAM-17 is critical for (PMA-induced) GH receptor proteolysis and GHBP generation. *Endocrinology.* **141**:4342–4348.
24. Diaz-Rodriguez, E., Montero, J.C., Esparis-Ogando, A., Yuste, L., and Pandiella, A. 2002. Extracellular signal-regulated kinase phosphorylates tumor necrosis factor alpha-converting enzyme at threonine 735: a potential role in regulated shedding. *Mol. Biol. Cell.* **13**:2031–2044.
25. Rio, C., Buxbaum, J.D., Peschon, J.J., and Corfas, G. 2000. Tumor necrosis factor-alpha-converting enzyme is required for cleavage of erbB4/HER4. *J. Biol. Chem.* **275**:10379–10387.
26. Bergmeier, W., et al. 2004. Tumor necrosis factor-alpha-converting enzyme (ADAM17) mediates GPIbalpha shedding from platelets in vitro and in vivo. *Circ. Res.* **95**:677–683.
27. Perou, C.M., et al. 2000. Molecular portraits of human breast tumours. *Nature.* **406**:747–752.
28. Shoyab, M., McDonald, V.L., Bradley, J.G., and Todaro, G.J. 1988. Amphiregulin: a bifunctional growth-modulating glycoprotein produced by the phorbol 12-myristate 13-acetate-treated human breast adenocarcinoma cell line MCF-7. *Proc. Natl. Acad. Sci. U. S. A.* **85**:6528–6532.
29. Martinez-Lacaci, I., et al. 1995. Estrogen and phorbol esters regulate amphiregulin expression by two separate mechanisms in human breast cancer cell lines. *Endocrinology.* **136**:3983–3992.
30. Schafer, B., Marg, B., Gschwind, A., and Ullrich, A. 2004. Distinct ADAM metalloproteinases regulate G protein-coupled receptor-induced cell proliferation and survival. *J. Biol. Chem.* **279**:47929–47938.
31. Giaccone, G., et al. 2004. Gefitinib in combination with gemcitabine and cisplatin in advanced non-small-cell lung cancer: a phase III trial--INTACT 1. *J. Clin. Oncol.* **22**:777–784.
32. Herbst, R.S., et al. 2004. Gefitinib in combination with paclitaxel and carboplatin in advanced non-small-cell lung cancer: a phase III trial--INTACT 2. *J. Clin. Oncol.* **22**:785–794.
33. Moore, M.J., et al. 2005. Erlotinib improves survival when added to gemcitabine in patients with advanced pancreatic cancer. A phase III trial of the National Cancer Institute of Canada Clinical Trials Group [NCIC–CTG]. In *American Society of Clinical Oncology Gastrointestinal Cancers Symposium*. January 27–29. Hollywood, Florida, USA. Abstract 77.
34. Shepherd, F.A., et al. 2005. Erlotinib in previously treated non-small-cell lung cancer. *N. Engl. J. Med.* **353**:123–132.
35. Lynch, T.J., et al. 2004. Activating mutations in the epidermal growth factor receptor underlying responsiveness of non-small-cell lung cancer to gefitinib. *N. Engl. J. Med.* **350**:2129–2139.
36. Paez, J.G., et al. 2004. EGFR mutations in lung cancer: correlation with clinical response to gefitinib therapy. *Science.* **304**:1497–1500.
37. Tsao, M.S., et al. 2005. Erlotinib in lung cancer — molecular and clinical predictors of outcome. *N. Engl. J. Med.* **353**:133–144.
38. Coussens, L.M., Fingleton, B., and Matrisian, L.M. 2002. Matrix metalloproteinase inhibitors and cancer: trials and tribulations. *Science.* **295**:2387–2392.
39. Egeblad, M., and Werb, Z. 2002. New functions for the matrix metalloproteinases in cancer progression. *Nat. Rev. Cancer.* **2**:161–174.
40. Beck, G., et al. 2002. (E)-2(R)-[1(S)-(Hydroxycarbamoyl)-4-phenyl-3-butenyl]-2'-isobutyl-2'-(methanesulfonyl)-4-methylvalerohydrazide (Ro 32-7315), a selective and orally active inhibitor of tumor necrosis factor-alpha convertase. *J. Pharmacol. Exp. Ther.* **302**:390–396.
41. Zhang, Y., et al. 2004. Characterization of (2R, 3S)-2-({[4-(2-butynyloxy)phenyl]sulfonyl}amino)-N,3-dihydroxybutanamide, a potent and selective inhibitor of TNF-alpha converting enzyme. *Int. Immunopharmacol.* **4**:1845–1857.
42. Garton, K.J., Ferri, N., and Raines, E.W. 2002. Efficient expression of exogenous genes in primary vascular cells using IRES-based retroviral vectors. *Biotechniques.* **32**:830, 832, 834 passim.